GESTO: a Glove for Enhanced Sensing and Touching Based on Inertial and Magnetic Sensors for Hand Tracking and Cutaneous Feedback

Tommaso Lisini Baldi, *Student Member, IEEE,* Stefano Scheggi, *Member, IEEE,* Leonardo Meli, *Member, IEEE,* Mostafa Mohammadi, *Student Member, IEEE,* and Domenico Prattichizzo, *Fellow, IEEE*

***Abstract*—The human hand represents a complex fascinating system with highly sensitive sensory capabilities and dexterous grasping and manipulation functionalities. As a consequence, estimating the hand pose and at the same time having the capability to provide haptic feedback in a wearable way may benefit areas such as rehabilitation, human-robot interaction, gaming, and many more. Existing solutions allow to accurately measure the hand configuration and provide effective force feedback to the user. However, they have limited wearability/portability. In this paper, we present the wearable sensing/actuation system GESTO (Glove for Enhanced Sensing and TOuching). It is based on inertial and magnetic sensors for hand tracking, coupled with cutaneous devices for the force feedback rendering. Unlike vision-based tracking systems, the sensing glove does not suffer from occlusion problems and lighting conditions. We properly designed the cutaneous devices in order to reduce possible interferences with the magnetic sensors and we performed an experimental validation on ten healthy subjects. In order to measure the estimation accuracy of GESTO, we used a high precision optical tracker. A comparison between using the glove with and without the haptic devices shows that the presence of them does not induce a statistically significant increase in the estimation error. Experimental results revealed the effectiveness of the proposed approach. The accuracy of our system, 3.32 degrees mean estimation error in the worst case, is comparable with the human ability of discriminating finger joint angle.**

***Index Terms*—Hand tracking, Haptic interfaces, Inertial and magnetic sensors, Cutaneous feedback, Wearable technology, Inertial measurement unit (IMU).**

I. Introduction

Capturing, analyzing, and interacting with the human body, and in particular with the human hands, is fundamental in several applications such as rehabilitation [1], human-robot interaction [2], and gaming [3]. In these contexts, wearability represents a key point since it improves the way humans interact with each others and the surrounding environment [4]. Wearable devices have the advantages of being portable and well integrated into people habits, with the aim of providing valuable information to the users. The idea is that technology will increasingly become more a consistent part of our daily life as it will be part of our clothing and sometimes even part of our bodies [5]. In the last years, there has been an increasing interest in developing new solutions to accurately track the human body and provide the users with realistic haptic feedback. However, most of the existing solutions are not completely wearable or portable. They usually rely on grounded devices and/or structured environments.

Concerning the human body tracking, several techniques were developed such as optical trackers, exoskeletons, camera-based tracking algorithms, and fabric-integrated sensors. Accurate optical tracking systems such as Vicon (Vicon Motion Systems, UK) and Optitrack (NaturalPoint Inc., USA) exploit active or passive optical markers to estimate the human body configuration with high precision and accuracy. The main

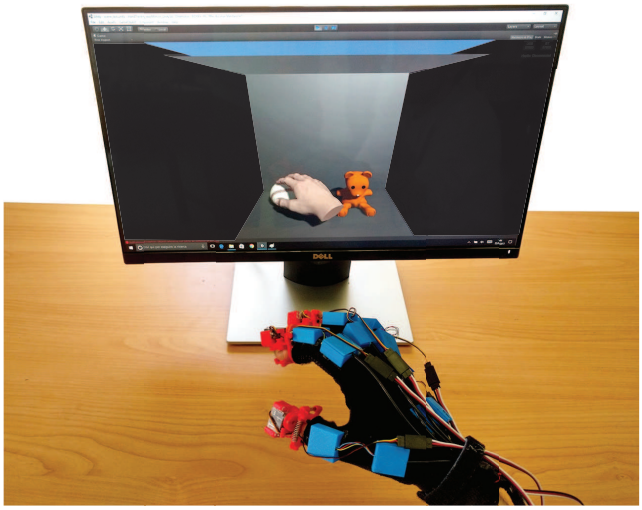

Fig. 1: GESTO (Glove for Enhanced Sensing and TOuching) in a gaming scenario. It is made by 11 MARG boards (blue) for sensing, and 5 wearable haptic devices (red) for force feedback. It allows to estimate the joints values and rotation of the human hand with respect to a global reference frame. Also, it can provide cutaneous haptic feedback to the user while interacting with virtual/remote environments. A modular solution is adopted in order to easily connect a different number of cutaneous devices as well as allowing to separately use the sensing and the actuation components.

T. Lisini Baldi, L. Meli, M. Mohammadi, and D. Prattichizzo are with the Department of Information Engineering and Mathematics, University of Siena, 53100 Siena, Italy, and with the Department of Advanced Robotics, Istituto Italiano di Tecnologia, Genova, 16163, Italy. {lisini, meli, mohammadi, prattichizzo}@{diism.unisi.it}

S. Scheggi is with the Surgical Robotics Laboratory, Department of Biomechanical Engineering, MIRA-Institute for Biomedical Technology and Technical Medicine, University of Twente, The Netherlands. s.scheggi@utwente.nl

The research leading to these results has received funding from the European Union Seventh Framework Programme FP7/2007-2013 under grant agreement n. 601165 of the project "WEARHAP - WEARable HxAPtics for humans and robots".

drawback of these approaches is the fact that these frameworks need a structured environment. Exoskeletons allow to accurately estimate the human pose thanks to their rigid structure and high quality sensors [6], [7]. Disadvantages result in cost and weight.

Although the aforementioned solutions provide very precise motion estimation, they are neither wearable/portable, nor usable in unstructured or outdoor scenarios. Towards the concept of portability, camera-based tracking algorithms became a widespread solution due to improvements in computer vision techniques and progressive growth in computers computational capabilities. In [8] and [9] the authors developed a hand tracker which employed a commercial RGB-D camera to extract the position, orientation, and configuration of the human hand. Commercial devices, like the Leap Motion (Leap Motion Inc., USA), allow to simultaneously estimate the full hand configurations of both hands. However, camera-based solutions have some limitations: RGB-D cameras might not work properly in an outdoor environment due to the infrared interference, and occlusions of the fingers may cause a poor estimation of the hand pose.

A viable solution consists in using fabric-integrated devices, e.g., datagloves based on piezoresistive, fiberoptic, magnetic, and Hall-effect sensors [10]. In [11] the authors developed a piezoresistive glove to measure the fingers flexion. An improved version, which included also abduction measurements, was presented in [12]. A wireless low-cost glove based on flexible resistive sensors was presented by Borghetti *et al.* [13]. This system was characterized by a low power consumption with a weekly battery lifetime. Recently, Bianchi *et al.* [14] built a prototype of a glove equipped with goniometers, which was capable of reconstructing the whole hand posture (with the exception of the palm's orientation) in grasping tasks. Despite the results, goniometer technology presents some limitations related to the high number of electrical connections per joint, which may reduce the wearability of the system. Different from camera-based trackers, data gloves require the users to wear additional equipment (such as gloves), which may prevent the users to have a natural interaction with the environment.

Another way to estimate the pose of the human body is to use Micro Electro-Mechanical Systems (MEMS) technology. In particular, a MARG (Magnetic, Angular Rate, and Gravity) board consists of a MEMS triaxial gyroscope, accelerometer, and magnetometer. The sensors board can be integrated with a wearable device and used to reconstruct the pose of the human body. The main drawback of MARG sensors is that the majority of the algorithms used to estimate their orientation rely on the magnetometer, thus they are sensitive to variations in the magnetic field. In spite of that, tracking systems based on this technology are commercially available and allow to accurately track the whole body, except the hands, both in outdoor and indoor environments, under different lighting conditions and free from grounded hardware [15]–[18]. Focusing on hands, a MARG tracking glove using 2-axis accelerometers was developed in [19]. The authors, by means of six sensors placed on the fingers, made a whole-hand input device exploiting the 26 postures of the american sign language alphabet. A similar device, using triaxial accelerometers, was developed by Kim *et al.* [20]. This device was used as a wearable mouse by allowing three fingers to operate as the left, middle, and right buttons. A sensing glove composed of inertial and magnetic sensors was proposed in [21]. For each finger, the authors used two pairs of triaxial gyroscope/accelerometer placed on the proximal and intermediate phalanges, and a triaxial magnetometer placed on the fingertip. The sensors were connected to multiple micro-controllers in order to achieve an accurate estimation. The proposed data glove used one sensors board for each phalanx, three MEMS sensors boards for the palm, and additional hardware to collect and process the data.

By considering all the aforementioned tracking methodologies, we focus on MEMS technology to estimate the hand pose. This choice fits the requirements of designing a wearable low cost sensing system capable of working in unstructured environments with varying lighting conditions. Moreover, since the goal is to provide also haptic feedback exploiting cutaneous devices, a glove instrumented with MARG sensors represents a good solution in terms of hardware integration, user customization, and tracking capability.

Concerning the haptic feedback, recently many haptic devices were designed to be portable and wearable by using vibrations and motor-driven platforms. Vibrotactile stimuli are usually generated by DC motors with eccentric masses, which can be easily integrated in devices like suits, bracelets, shoes, gloves, etc [22]–[24]. Although vibrotactile stimuli have been successfully used to guide the human motion [25]–[27], they can only provide multi-frequency patterns, with a limited force feedback rendering capability.

Motor-driven platforms devices use DC motors [28] or servomotors [29] to tilt a mobile platform and render 3-D forces on the finger pads. The idea behind these devices originates from the observation that stimuli received by the user, while interacting with an object, consist also of a cutaneous sensation perceived by mechanoreceptors in the skin. Previous researches demonstrated the potential of these interfaces in recognizing the local properties of objects, such as shape and edges [28]. Due to their reduced size, these devices can be integrated with an RGB-D tracker or with a Leap Motion controller in order to provide haptic feedback in virtual reality interaction [30], [31].

In this work, we use wearable cutaneous devices which provide force feedback via motor-driven platforms. Even if vibrotactile motors represent a more wearable solution, cable-spring driven devices can generate a more realistic feeling of touch. To make the haptic interfaces more wearable, comfortable, and compatible with the proposed tracking glove, we design a custom version of the devices presented in [29] and [31].

Our contribution consists in presenting GESTO (Glove for Enhanced Sensing and TOuching) based on MARG sensors for hand tracking and cutaneous devices for force feedback (Fig. 1). The sensing glove can estimate the joints values of the hand as well as its rotation with respect to a global reference frame. To the best of our knowledge, this represents one of the first attempts to combine a sensing glove based on inertial and magnetic sensors with haptic tactile devices. A possible disadvantage of combining magnetometer and motor-driven devices

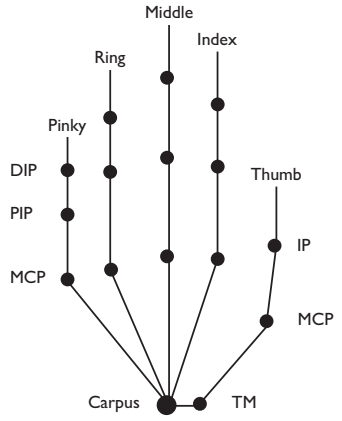

Fig. 2: A simplified kinematic structure of the human hand having 23 Degrees of Freedom (DoFs): 4 DoFs for each finger (two for the first joint and one for each of the remaining joints) and 3 DoFs for the hand rotation.

consists in having permanent magnet inside the devices that might affect the performance of the magnetic sensors. To overcome this limitation, we design the glove in order to take advantage of the biomechanical constraints of the human hand [32], [33]. To the best of our knowledge, our results represent the first experimental demonstration of the use of MARG sensors coupled with cutaneous devices that simultaneously, (1) estimate the orientation and configuration of the hand and (2) provide haptic feedback to the user. Different from existing solutions, the proposed system is wearable, portable and it can be used in indoor/outdoor unstructured environments. This work is based on previous conference material [34] compared to which we provide herein a new and improved prototype of the sensing glove, a new haptic device, a more extended theory, and a more comprehensive experimental validation.

The rest of the paper is organized as follows. Sect. II presents the kinematic model of the hand used in this work. Sect. III describes the proposed sensing glove and the tracking algorithm used to estimate the hand pose. Sect. IV shows the cutaneous haptic devices used for the force rendering. Sect. V reports the results of the experimental validations, whereas in Sect. VI conclusions and possible subjects of future research are outlined.

II. Hand modeling

In what follows, we present the simplified kinematic model of the hand, which will be instrumental in the design of the sensing glove. A complete human hand model has about 30 degrees of freedom (DoFs) [35]. For the sake of simplicity and without loss of generality, we use a simplified kinematic hand structure. We model each finger as a planar kinematic chain, with one universal joints (two intersecting, orthogonal revolute joints) and two one-dimensional hinges. In accordance with [36], we assume that each finger has the metacarpal (MC) bone fixed with respect to the hand frame, and characterized by four DoFs. In a more complete model of the human hand, the thumb has at least five DoFs: two in the trapeziometacarpal (TM) joint, two in the metacarpophalangeal (MCP) joint and one in the interphalangeal (IP). However, the abduction/adduction motion range of the MCP joint usually can be neglected and the thumb can be modeled with four DoFs. Index, middle, ring, and pinky fingers have two DoFs in the MCP joint (one for adduction/abduction and another for flexion/extension), one in the proximal interphalangeal (PIP) and one in the distal interphalangeal (DIP). Fig. 2 shows the model of the hand used in this work. Each finger is modeled using four parameters, two for the rotation of the first joint and two for the remaining joint angles. The orientation of the palm is represented using quaternions. The hand model has 23-DoFs identified by 24 parameters, i.e., 20 values for the joints of the fingers and a quaternion for the palm orientation.

TABLE I: Static constraints of the fingers.

Digit	Joint	Flexion (deg.)	Extension (deg.)	Abduction Adduction (deg.)
Thumb	TM	90	15	60
	MCP	80	0	0
	IP	80	10	0
Index	MCP	90	40	60
	PIP	110	0	0
	DIP	90	5	0
Middle	MCP	90	40	45
	PIP	110	0	0
	DIP	90	5	0
Ring	MCP	90	40	45
	PIP	120	0	0
	DIP	90	5	0
Pinky	MCP	90	40	50
	PIP	135	0	0
	DIP	90	5	0

Even if the human hand is extremely articulated, movements of the fingers are constrained to a specific range due to dynamic and static constraints. Static constraints refer to the limit of the range of finger motions as a result of the hand anatomy. Dynamic constraints are referred to the limits on the joints during motions. This typology can be divided in two groups, inter-finger and intra-finger constraints. Inter-finger constraints refer to the ones imposed on the joints values between different fingers. Intra-finger constraints relate the joints of the same finger. These constraints were studied by Cobos *et al.* in [32].

Recently, the authors enhanced the previous results with the following relationship for the index, middle, ring, and pinky [33],

$$\theta_{DIP} \simeq 0.88\, \theta_{PIP} \tag{1}$$

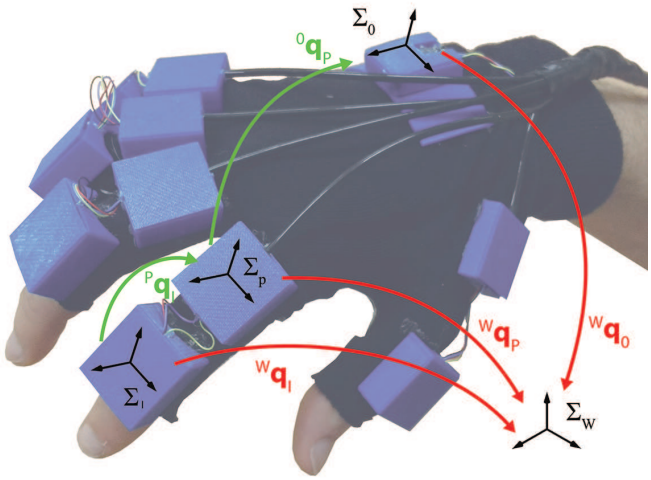

Fig. 3: Coordinate frames and quaternion that express the orientation used for the MARG tracking system. In green is reported the orientation of the intermediate phalanx referred to the proximal phalanx ${}^{P}\mathbf{q}_I$, and the orientation of the proximal phalanx with respect to the palm ${}^{0}\mathbf{q}_P$. phalanx ${}^{W}\mathbf{q}_I$, proximal phalanx ${}^{W}\mathbf{q}_P$, and palm ${}^{W}\mathbf{q}_0$ with respect to the world frame Σ_W.

and

$$\theta_{IP} \simeq 0.77\, \theta_{MCP} \tag{2}$$

for the thumb. The authors found also that neither the hand position, nor the used hand (left/right) had an influence on the linear relationship between the two distal finger joint angles. Static constraints on the values of each joint are based on anatomical studies [32], [37]. Table I reports the static constraints used in this work. Note that intra-finger constraints are used to design the glove in order to minimize the number of MARG sensors while allowing its integration with cutaneous haptic devices. Static constraints are used by the tracking algorithm in order to provide a correct estimation of the human hand.

III. Design of the Sensing Glove and Hand Tracking Algorithm

The cutaneous devices considered in this work are assumed to be rigidly attached to the distal phalanges of the fingers as the ones developed in [28]. Thus, we design a sensing glove made by 11 MARG sensors (1 sensor for the palm and 2 sensors for each finger) and we exploit the biomechanical constraints reported in Sect. II. For all the fingers, we place the sensors on the intermediate and proximal phalanges and we model the relation between the upper finger joints, as described in Eqs. (1)-(2). Each MARG board [1] contains a triaxial accelerometer/gyroscope (InvenSense MPU6050) and a triaxial magnetometer (Honeywell HMC5883L). Ten sensors boards are placed on the dorsal surface of the fingers and one on the back of the palm (Fig. 3). The last phalanx of each finger is left uncovered to not affect the user's tactile perception. The sensing glove uses an Arduino Nano with an ATmega328 microcontroller. Arduino collects the raw data from the MARG boards, and sends them through an 115200 bps serial connection to an external computer in charge of all the mathematical computations. The update rate of the system is 50 Hz. In particular, the accelerometer sample rate is 1 kHz, the gyroscope can provide an 8 kHz output data rate, whereas the magnetometer can achieve a maximum rate of 160 Hz in single measurement mode and 75 Hz in continuous measurement mode. The glove is designed by considering the 50^{th} percentile of European men and women, age 20-50. This is a very common approach in objects design and ergonomics. The housing of the sensors is designed in order to fit the finger and narrow the possible movements of the electronic board as the hand/fingers move. In what follows, we describe the procedure to calibrate the sensing glove and the hand tracking algorithm based on MARG sensors.

[1]Board refers to electronic board that contains the sensors and other necessary electronic components.

A. Calibration of the sensing glove

Each MARG sensor requires an initial calibration (see the Appendix for further details). The tracking algorithm requires an initial setup, which consists of three steps. In the first step, the user is asked to displace the hand in a known *a-priori* position, e.g., the user places the hand in a flat surface. In this phase, each MARG sensor collects 200 samples to estimate the gyroscope bias. In the second step, for each hand joint we compute the offset quaternion combining the joint estimations and the known posture. In the last step, similarly to [15], we use the *a-priori* knowledge of the hand kinematic chain to estimate the length of the links. The user is asked to touch in turn the fingertip of the thumb with the fingertip of the other fingers (index, middle, ring and pinky) and moving them without applying forces to the finger pads, to not violate the constraint in Eq. (1). Since the distance between the fingertip is zero, we can take advantage of the kinematic chain to improve the estimation of the length of the bones. Starting from an initial value (taken from anthropometric measurements), we perform an optimization algorithm to refine the estimation. The *a-priori* lengths of the fingers are used as a starting point to initialize the optimization problem that minimizes the distance between the two fingertips. We validate this procedure with synthetic data. This is a common approach in the relevant literature when accurate measurements are hard to obtain [8]. We performed 30 trials. For each trial we generate hand configurations with pseudo-random lengths of the phalanges and joints values (an admissible range of values is considered). Joints values are corrupted with zero mean Gaussian noise with a standard deviation of 3 deg, simulating the estimation error of the MARG sensors (Sect. V). The optimization procedure estimates the length of the phalanges with an error less then 5% of the real bone length.

B. Hand tracking algorithm

In what follows, we report the joint estimation for a generic finger, since the same approach applies to all fingers. Let

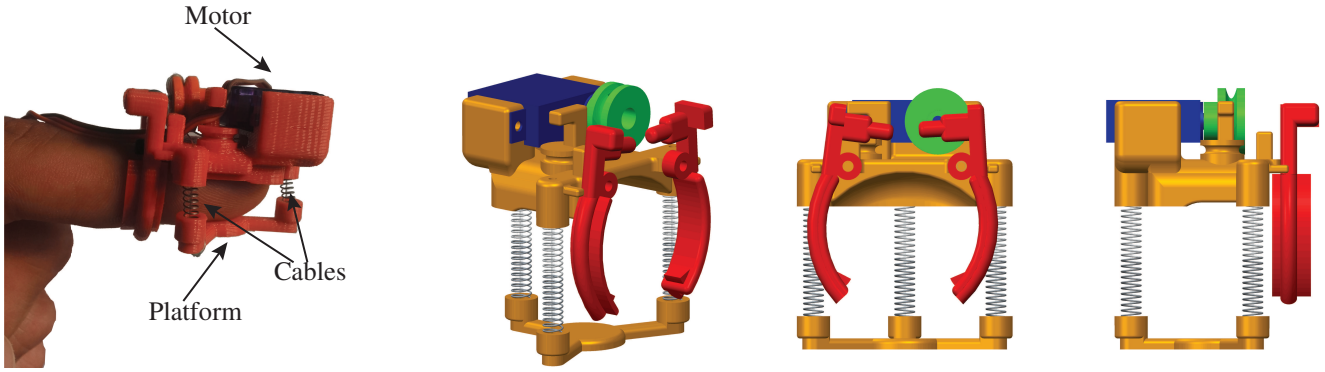

(a) (b)

Fig. 4: The wearable cutaneous device is composed of two platforms (a): one placed on the nail side of the finger and one in contact with the finger pad. One small servomotor controls the length of three cables in order to display the desired force to the user. The rendered 3-D model of the device from three different points of view is reported in (b).

${}^{W}\mathbf{q}_0(t)$, ${}^{W}\mathbf{q}_P(t)$, ${}^{W}\mathbf{q}_I(t)$ be the quaternions that express the orientation, with respect to the global reference frame Σ_W, of the frames associated to the palm, to the proximal phalanx, and to the intermediate phalanx (Fig. 3). Let ${}^{0}\hat{\mathbf{q}}_P$ be the offset quaternions between the proximal phalanx and the palm, and ${}^{P}\hat{\mathbf{q}}_I$ the offset quaternion between the intermediate phalanx and the proximal one, both estimated during the aforementioned calibration phase. The orientation of the proximal phalanx referred to the palm can be computed as

$$ {}^{0}\mathbf{q}_P(t) = {}^{0}\mathbf{q}_W(t) \otimes {}^{W}\mathbf{q}_P(t), $$

where ${}^{0}\mathbf{q}_W(t)$ is the conjugate quaternion of ${}^{W}\mathbf{q}_0(t)$. Then, the quaternion which describes the rotation of the proximal phalanx with respect to the initial configuration results

$$ \mathbf{q}_P(t) = {}^{P}\hat{\mathbf{q}}_0 \otimes {}^{0}\mathbf{q}_P(t). \tag{3} $$

The quaternion $\mathbf{q}_P(t)$ is converted to the Euler angles representation and used to compute the flexion/extension and abduction/adduction values of the MCP joint. In the same way, the orientation of the intermediate phalanx with respect to the proximal phalanx is estimated

$$ {}^{P}\mathbf{q}_I(t) = {}^{P}\mathbf{q}_W(t) \otimes {}^{W}\mathbf{q}_I(t) $$

and consequently,

$$ \mathbf{q}_I(t) = {}^{I}\hat{\mathbf{q}}_P \otimes {}^{P}\mathbf{q}_W(t) \otimes {}^{W}\mathbf{q}_I(t). \tag{4} $$

Then, the Euler angles conversion is used to compute the value of the PIP joint. Finally, the value of the DIP joint is obtained from the estimated values of the PIP joint, exploiting (1). For the orientation estimation of each MARG sensor with respect to the global world frame Σ_W, we use the algorithm proposed in [38] since it achieves the lowest estimation error (see Sect. V) and it has only one parameter to be set (see the Appendix).

IV. Design of the Wearable Haptic Devices

Contextually with the tracking glove, we present the cutaneous devices for cutaneous feedback. Cutaneous devices received an increasing interest in the last years, due to the possibility to provide haptic feedback in a wearable way, and thus contribute in bringing haptic technologies to everyday life applications. Minamizawa *et al.* [39] found that the deformation of the finger pads due to the interaction with an object can generate a reliable sensation even when perceptions on the wrist and arm are absent. This implies that a simple device for reproducing the virtual object can be realized by recreating the finger pad deformation. Based on these observations Pacchierotti *et al.* [4] presented a 3-DoFs wearable cutaneous haptic device able to provide cutaneous stimuli at the finger pad. The device was made of a body that contained three servomotors (placed on the fingernail) and a mobile platform that applied the required forces. To have a more compact, wearable, and suitable solution for the tracking systems, Scheggi *et al.* [31] developed a smaller 1-Dof device for the force feedback rendering. The device was composed of two platforms: one placed on the nail side of the finger and one in contact with the finger pad. Three cables and three springs connected the two parts, while one small servomotor controlled the length of the cables. The idea was to move the platform towards or away from the finger pad, to display a force at the user's fingertip.

In this study, we improve the design presented in [31]. We change shape and weight (reduced to 12.6 g) of the cutaneous device to optimize its use with the sensing glove. The size of the device is minimized and the motor (Hitec HS5035-HD Digital Ultra Nano) is moved from the back of the device to the front, positioning it horizontally in order to remove the magnetic disturbance affecting the MARG sensors (Fig. 4).

A. Haptic feedback

At the equilibrium static condition, the force induced by the finger pad is balanced with the forces generated by the three cables. For each cable the resultant force can be expressed as the sum of two components. The first one is the force generated by the servomotor, and its module depends on the motor torque. The second one is the resistance given by the three springs, and the module depends on the springs stiffness.

This force is expressed with respect to the center of the platform and results

$$F_f = \left(\frac{\tau}{r} - 3k_s|d - d_0|\right),$$

where τ is the motor torque (max 0.078 Nm for the servomotor used), $r = 0.0055$ m is the pulley radius, $k_s = 300$ N/m is the springs stiffness, d is the current cable length, and d_0 is the nominal spring length ($d_0 = 0.015$ m). Therefore, to generate the desired force we start from an initial position in which: (i)the fingertip is not stimulated by the device, and (ii) the platform is in contact without producing skin deformation. This position is reached using a preliminary manual calibration. The use of a force sensor on the platform would make this procedure automatic, but it would also add extra wires, thus increasing the complexity of the device to wear. Since the finger pad is compliant, the displacement of the platform produces a deformation of the finger pulp that leads to a contact stress distribution. Thus, a relationship between the position of the platform and the exerted force can be evaluated.

In order to describe this ralationshop, let us recall some of the mathematical and numerical models for the human fingertip which have been proposed in the literature. In [40] a study on structural model of the fingertip was presented. The paper took into account both the material in-homogeneity and geometry. The authors studied whether the proposed fingertip model could predict the force-displacement and the area responses of relative force during interaction with a flat, rigid surface, like our platform. Moreover, they evaluated if the stresses and strains predicted by this model were consistent with the tactile sensation. In [41] the authors presented a 2-D continuum fingertip model. The finger was approximated by an homogeneous, isotropic and in-compressible elastic material. The undeformed fingertip was modeled as an axial symmetric ellipsoidal elastic membrane, filled with a in-compressible fluid with an internal pressure. The authors considered a 2-D model and an external load was applied to the finger through a flat surface. The model predicted a pulp force/displacement relationship which could be represented as a non linear hardening spring, i.e., whose stiffness increased with the applied load. In [42], Wu *et al.* described a 2-D finite element model of the fingertip. The skin was modeled as an hyper-elastic and viscoelastic membrane, and the subcutaneous layer was considered as a biphase material. Thus, fingertip deformation and applied force could be related by an impedance model, which was non-linear and depends on the fingertip specific characteristics (e.g., the subject age). Because of the simplicity of the 1-DoF devices used in this paper, we consider a simplified model of the fingertip, i.e., a linear relationship between resultant normal force and platform displacement. The isotropic elastic behavior of the finger pad with stiffness $K_f = 0.5$ N/m considered here is in accordance with the work of Park *et al.* [43]. In other terms, we assume that the platform displacement is proportional to the desired force F_p to be applied to finger pad by the mobile platform,

$$\Delta p = K_f^{-1} F_p,$$

where Δp is the displacement of the platform with respect to its initial position, i.e., when the platform is in contact with the finger pad without producing any skin deformation. Because of the design of the device, and the possible maximum displacement of the platform, the maximum force that can be provided to the human's finger pad is about 5.2 N. A similar open-loop control of wearable cutaneous devices was used in [4] and [28] for 3-DoF cases.

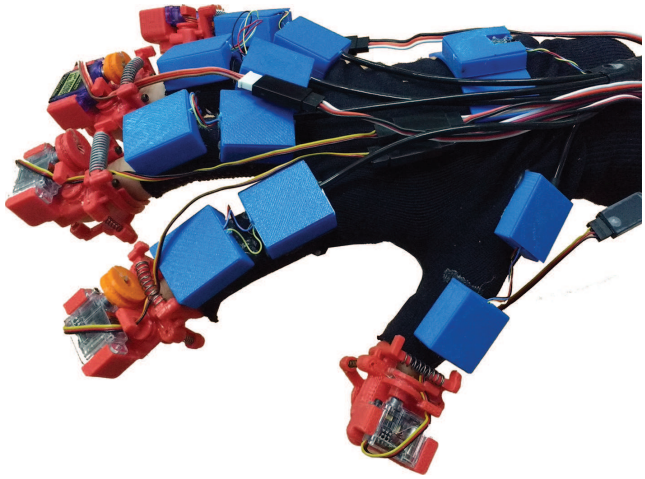

Fig. 5: GESTO (Glove for Enhanced Sensing and TOuching) is composed of 11 MARG sensors (blue): 1 sensor for the palm and 2 sensors for each of the remaining fingers. 5 wearable haptic devices (red) provide force feedback to the user.

TABLE II: Mean and standard deviation of the attitude estimation error for the four considered algorithms.

Algorithm	Roll (deg.)	Pitch (deg.)	Yaw (deg.)
GN	2.70 ± 1.83	1.42 ± 1.13	2.47 ± 1.68
NCF	2.68 ± 1.76	1.43 ± 1.13	2.58 ± 1.72
GDC	2.71 ± 1.94	1.58 ± 1.23	2.63 ± 3.24
GNK	2.84 ± 2.46	2.08 ± 2.03	3.24 ± 3.25

V. Experimental validation

In this section we report the experimental validation of the proposed system (Fig. 5). The total weight of the glove is 160.5 g, including the Lycra-glove (72 g), 5 devices (12.6 g each), and cables (25.5 g). A preliminary experiment was conducted to test the performance of four attitude estimation algorithms. Additional experiments were performed to prove the robustness, dynamic performance, precision, and compatibility of the proposed sensing glove with the wearable haptic devices[2].

A. Experimental comparison of the attitude estimation algorithms

We tested and implemented four different algorithms for the orientation estimation of MARG sensors:

[2]Please notice that this paper is accompanied by multimedia material. A video is available also at: http://goo.gl/3AChOR.

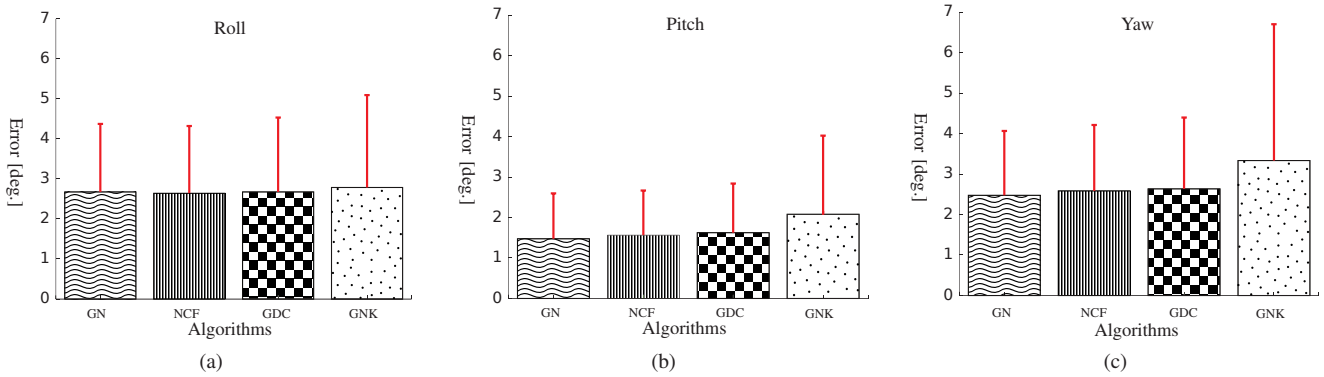

Fig. 6: *Comparison among the four different estimation algorithms.* The MARG sensor was freely moved and rotated. An accurate optical tracking system was used to compute the ground truth measurements. For each algorithm we report the mean and standard deviation of the error in orientation estimation expressed as roll, pitch and yaw angle.

i Gauss-Newton method (GN) combined with a complementary filter [38];
ii Nonlinear Complementary Filter (NCF) suggested by Mahoney [44];
iii Gradient descent algorithm coupled with a complementary filter (GDC), proposed by Madgwick [45];
iv Gauss-Newton method with Extended Kalman Filter (GNK) in a quaternion version [46].

In order to compare the algorithms, we used an accurate optical tracking system, whose output was considered as ground truth reference. A Vicon tracking system consisting of 8 cameras was used to provide reference measurements of the MARG sensor orientation. The sensor was placed on a flat platform together with six passive optical markers. An initial calibration procedure was performed in order to align the reference frame of the sensor with the one of the Vicon.

We freely moved and rotated the platform, 10 trials were performed. Each trial was 90 seconds.

A comparative error analysis among the four algorithms is reported in Table II and Fig. 6. In Fig. 7 we report the ground truth values of a typical trial. The estimated quaternions are transformed in Euler angles only for the sake of clarity. In the proposed system, we used the algorithm presented in [38] since it achieved the lowest estimation error, and it had only one parameter to be set.

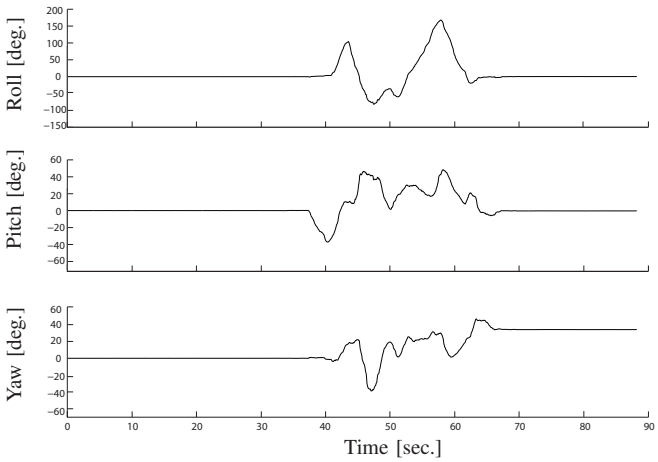

Fig. 7: *Experiment 1.* The MARG sensor was positioned onto a flat platform together with six passive optical markers. We kept the platform steady for 30 seconds, then we freely moved and rotated it for 30 seconds, and finally we kept it steady for further 30 seconds. A representative trial is depicted; only the orientation estimated by the optical tracker is reported.

B. Experimental validation of the sensing glove

In this section, we report the results concerning the validation of the hand posture estimated by the proposed sensing glove. We firstly validate the glove without the wearable haptic devices, then we discuss the results of the test conducted wearing the devices. Finally, we compare these results using the statistical analysis in order to demonstrate the robustness of the proposed system. Ten healthy subjects were involved in the first experiment (age range 24-47, 8 males and 2 females, all right-handed). None of the participants reported any deficiencies in the perception abilities (including vision, hearing, touch and proprioception). The participants signed informed consent forms. All of them were informed about the purpose of the experiment, were able to discontinue participation at any time and no payment was provided for the participation. Each user was asked to wear the glove and freely move his/her right hand for 90 seconds without any training session. Two trials for each subject were performed.

We recorded the users' hand configuration both using our sensing glove and the Vicon tracking system. On each MARG we placed four passive markers and processed at the same time the orientation computed by the optical tracking system and by the inertial and magnetic sensors. For each subject we computed the values of the fingers' joints both with the MARG boards and the optical tracker (cf. Sect. III). A representative joint angle values estimation is shown in Fig. 8.

Table III summarizes the first experimental results. The table reports the average error and the 95% Confidence Interval for all the considered joints of the hand among the different trials of the users: the mean of the estimation error is less than 3.30

degrees for all the considered joints, thus the accuracy of the system is close to the human ability in discrimination of finger joint-angle [47].

Then, to evaluate the compatibility of the proposed glove with the wearable haptic devices we performed the same experimental procedure wearing the haptic interfaces. Ten healthy subjects (age range 24-47, all males and right-handed) were involved in this test. None of the participants reported any deficiencies in the perception abilities (including vision, hearing, touch, and proprioception). The participants signed informed consent forms. All of them were informed about the purpose of the experiment, were able to discontinue participation at any time, and no payment was provided for the participation. Each user was asked to wear the full system (glove and five haptic devices) and move his/her right hand for 90 seconds. Two trials without any training session were performed for each user. No specific task or gesture was suggested. The motors received a sinusoidal input signal to continuously move up and down the platform and generate a variable magnetic field and soft iron disturbance.

Table IV reports the average error and the 95% Confidence Interval for the PIP joint values for each finger, and MCP for the thumb. It reports also the estimated values for the MCP joint for index, middle, ring, pinky, and (TM for the thumb). This experiment reveals that the interference effect generated by the motors is negligible for the joint values estimation.

To prove and validate these results we perform a statistical

TABLE III: Mean and 95% Confidence Interval of the joint estimation error without haptic devices. The data are computed among ten users; each user performed two trials.

Digit	Joint	Error (deg.)	Confidence Interval 95% (deg.)
Thumb	TM (F/E)	3.20	[3.08 3.32]
	TM (A/A)	2.87	[2.76 2.98]
	MCP	3.72	[3.57 3.86]
Index	MCP (F/E)	3.62	[3.49 3.75]
	MCP (A/A)	3.27	[3.16 3.38]
	PIP	3.16	[2.98 3.34]
Middle	MCP (F/E)	2.73	[2.60 2.86]
	MCP (A/A)	2.68	[2.57 2.77]
	PIP	2.66	[2.56 2.76]
Ring	MCP (F/E)	2.98	[2.85 3.11]
	MCP (A/A)	3.20	[3.09 3.32]
	PIP	3.04	[2.89 3.19]
Pinky	MCP (F/E)	2.72	[2.60 2.83]
	MCP (A/A)	2.97	[2.86 3.08]
	PIP	3.16	[3.02 3.30]

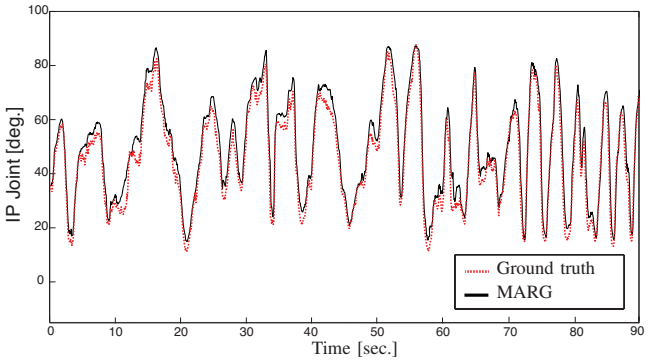

(a)

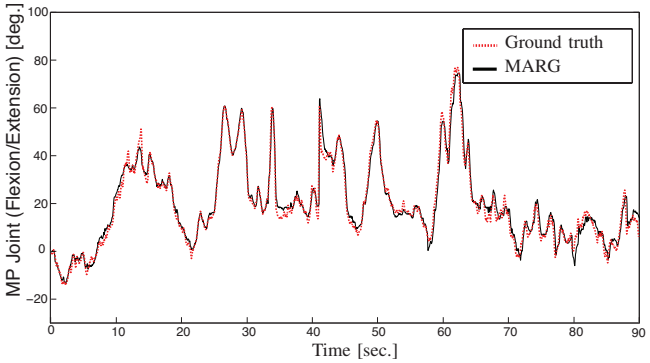

(b)

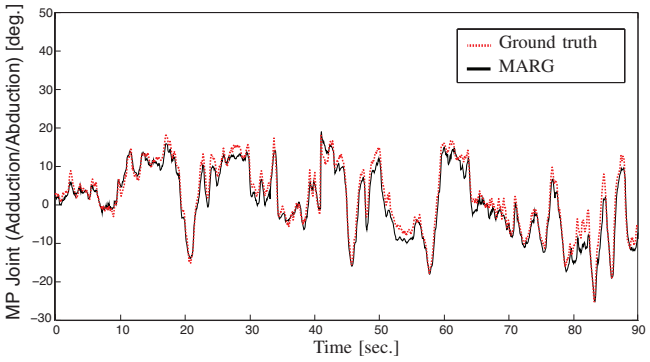

(c)

Fig. 8: Joint orientation estimation for the index finger, representative user.

analysis on the data, analyzing the error in the orientation estimation (dependent variable) under the two different conditions, the glove coupled or not with the devices. We exploit the paired sample t-test to determine whether the mean difference between paired observations is statistically significant. We process the data recorded in the two experimental sessions.

Firstly, we validate the hypothesis that the presence of the devices is negligible for the estimation of the MCP joints orientation. We take into account the worst case, i.e., the pinky. Indeed, since it has the shortest link compared to the other fingers, the distance between the MARG sensor and the device is the smallest one. Collected data passed the Shapiro-Wilk normality test ($p = 0.662$) and a comparison of the means among the error is carried out. The presence of the haptic interfaces does not elicit a statistically significant

TABLE IV: Mean and 95% Confidence Interval of the joint estimation error when the wearable haptic devices are used. The data are computed among ten users; each user performed two trials.

Digit	Joint	Error (deg.)	Confidence Interval 95% (deg.)
Thumb	TM (F/E)	4.68	[4.43 4.91]
	TM (A/A)	4.64	[4.45 4.83]
	MCP	3.11	[2.98 3.24]
Index	MCP (F/E)	3.21	[3.07 3.36]
	MCP (A/A)	2.89	[2.76 3.02]
	PIP	3.26	[3.10 3.42]
Middle	MCP (F/E)	2.28	[2.14 2.41]
	MCP (A/A)	2.84	[2.69 2.98]
	PIP	2.15	[2.02 2.28]
Ring	MCP (F/E)	3.23	[3.10 3.36]
	MCP (A/A)	2.41	[2.31 2.50]
	PIP	4.73	[4.58 4.88]
Pinky	MCP (F/E)	3.47	[3.32 3.62]
	MCP (A/A)	2.50	[2.64 2.37]
	PIP	4.93	[4.74 5.10]

increase in error compared to the estimation without them ($t(19) = 0.876,\ p = 0.410$).

Once the relationship between the haptic devices and the sensors placed on the proximal phalanx is investigated, we focus our attention on the sensors boards placed close to the motors. Three statistical analyses for this scope are performed. In the former, we analyze the error among all the PIP joints, in the second we carry out the test only for the PIP joint of the pinky, whereas in the latter we focus our attention on the intermediate phalanx of the ring. The first analysis is used to determine whether there is a statistically significant mean difference between using the glove with and without the haptic devices. The assumption of normality was not violated, as assessed by Shapiro-Wilk's test ($p = 0.714$). The test reveal that wearing the haptics interfaces does not induce a statistically significant increase in estimation error ($t(99) = 1.452,\ p = 0.154$). In the second and third analysis, we investigate whether the presence of the device worn on the pinky produces a statistically significant mean increase in error estimation for the boards placed on the second phalanx of the ring and of the pinky. Because of the shortest bones of the pinky, these sensors are the closest to the device, compared to all the other possible motor-sensor distances. Results of a paired sample t-test reveal that the mean difference was statistically significant only for the pinky PIP estimation ($t(19) = 2.642,\ p = 0.033$), whereas we can reject this hypothesis for the ring ($t(19) = 2.022,\ p = 0.083$).

VI. Conclusions and future work

Estimating the human hand pose and, at the same time, having the capability to provide haptic feedback in a wearable way is a challenging task. In this paper, we present a possible solution which relies on MARG sensors for the pose estimation, and cutaneous haptic devices for the force feedback. The proposed device GESTO (Glove for Enhanced Sensing and TOuching) can estimate the joints values of the hand as well as the hand rotation with respect to a global reference frame. It is designed to limit possible disturbances that may arise between the magnetometers of the MARG sensors and the servomotors of the haptic interfaces. A modular solution is considered to connect an arbitrary number of cutaneous devices as well as allowing to separately use the sensing and the actuation components. The experimental validation conducted on ten healthy subjects revealed that the 95% confidence interval for the orientation estimation error is 3.06 ± 0.12 degrees among all the hand joints without the devices and 3.32 ± 0.15 degrees with the devices. These experiments demonstrate the possibility to sense and provide force feedback to the human hand in a wearable and portable way.

As part of future work, we will improve GESTO by using customized and flexible sensing boards of smaller size to better fit also smaller-sized hands. Additional studies will be performed in order to integrate the sensing glove with motor-driven platforms capable of applying 3-D forces on the finger pads. Furthermore, additional algorithms will be investigated and designed in order to reduce the estimation error of the system. Finally, we are working to make the system completely wireless. In order to save the battery life of the device, we plan to perform all the computations on an external computer and use a low performance micro-controller on the glove.

Appendix: orientation Estimation of MARG Sensors

In this section, we briefly detail the orientation estimation algorithm used in this work. We exploit the quaternion based method presented by Comotti in [38]. The author used quaternions to estimate the orientation of a single MARG sensor with respect to a global reference frame. Using quaternion allow us to overcome the problems introduced by the Euler angles, for instance the *gimbal lock* problem and the issues related to the trigonometric functions. In this algorithm and in the entire work we use the following convention to represent a quaternion: $\mathbf{q} = [\omega\ x\ y\ z]$, where ω is the real number. The proposed algorithm is composed of three parts, the former estimates the orientation relying on accelerometer and magnetometer measures, the second produces an estimation based on the gyroscope angular rate integration, and the latter fuses the two previous estimations. In the first part, the algorithm estimates the orientation using accelerometer and magnetometer measures, by minimizing a cost function. By exploiting the Gauss-Newton method, the algorithm processes

the measurement of gravity and Earth's magnetic flux to evaluate the actual sensor orientation. Let ${}^{S}\mathbf{a}(t)$, ${}^{S}\mathbf{m}(t) \in \mathbb{R}^{3\times 1}$ be the accelerometer and magnetic measures with respect to the sensor reference frame Σ_S. The Earth reference vector ${}^{S}\mathbf{z}(t)$, expressed in the sensor frame, results

$$ {}^{S}\mathbf{z}(t) = \begin{bmatrix} {}^{S}\mathbf{a}(t) \\ {}^{S}\mathbf{m}(t) \end{bmatrix} \in \mathbb{R}^{6\times 1}. $$

Using the same notation, we indicate the reference vector in the world reference frame Σ_W as

$$ {}^{W}\mathbf{z}(t) = \begin{bmatrix} {}^{W}\mathbf{a}(t) \\ {}^{W}\mathbf{m}(t) \end{bmatrix} \in \mathbb{R}^{6\times 1}. $$

Taking into account that the gravity vector is always aligned with the world z-axis, therefore we can consider

$$ {}^{W}\mathbf{z}(t) = \begin{bmatrix} 0 \\ 0 \\ 1 \\ {}^{W}\mathbf{m}(t) \end{bmatrix} \in \mathbb{R}^{6\times 1}. $$

Let the orientation estimation error be

$$ \epsilon(t) = {}^{W}\mathbf{z}(t) - {}^{W}\mathbf{M}_S(t)\, {}^{S}\mathbf{z}(t) \tag{5} $$

where ${}^{W}\mathbf{M}_S(t) \in \mathbb{R}^{6\times 6}$ indicates the rotation matrix between the sensor frame Σ_S and the world frame Σ_W. The role of the algorithm is to minimize ϵ, i.e., estimate ${}^{W}\mathbf{M}_S(t)$. Let $\mathbf{q}(t)$ be the quaternion representation of the rotation matrix ${}^{W}\mathbf{R}_S(t)$, a single step of the Gauss-Newton optimization method in a quaternion form produces

$$ \mathbf{q}_{i+1}(t) = \mathbf{q}_i(t) - \mathbf{J}_i^{\dagger}(t)\epsilon(t) \tag{6} $$

where

$$ \mathbf{J}_i^{\dagger}(t) = (\mathbf{J}_i^T(t)\mathbf{J}_i(t))^{-1}\mathbf{J}_i^T(t). $$

The subscript i represents the *i-th* iteration of the optimization algorithm and $\mathbf{J}_i(t)$ is the Jacobian of the error $\epsilon(t)$ reported in Eq. (5). Moreover, as recommended in [38] and [45] we include a compensation of the magnetic distortion.

In the second phase of the algorithm, an estimation based on the gyroscope measure is obtained. For each cycle the algorithm acquires from the sensor the angular rates ${}^{S}\omega_x(t)$, ${}^{S}\omega_y(t)$ and ${}^{S}\omega_z(t)$ referred to the $x-$, $y-$ and $z-$axis of the sensor frame Σ_S. These measures can be represented in the quaternion form

$$ {}^{S}\boldsymbol{\omega}(t) = 0 + \boldsymbol{i}\,{}^{S}\omega_x(t) + \boldsymbol{j}\,{}^{S}\omega_y(t) + \boldsymbol{k}\,{}^{S}\omega_z(t). $$

We consider

$$ {}^{S}\dot{\mathbf{g}}(t) = \frac{1}{2}\Big({}^{S}\mathbf{g}(t-\delta t) \otimes {}^{S}\boldsymbol{\omega}(t)\Big), \tag{7} $$

the rate of changing in orientation expressed as a infinitesimal quaternion variation, where ${}^{S}\mathbf{g}(t-\delta t)$ is the latest estimated quaternion, ${}^{S}\boldsymbol{\omega}(t) = [\ 0\ {}^{S}\omega_x(t)\ {}^{S}\omega_y(t)\ {}^{S}\omega_z(t)\ ]^T$ is the angular rate vector at the current time, $\otimes$ is the quaternion product, and δt is the sampling time.

The last step of the estimation algorithm fuses the quaternions estimated in the previous phases. A complementary filter is used to combine the two values. On the short term, the filter prefers the data from the gyroscope, whereas on the long term, it gives the greater gain to the data from the accelerometer, as it does not drift. The filter, by using two gain factors whose sum is 1, fuses the gyroscope quaternion $\mathbf{g}(t)$ with the quaternion $\mathbf{q}(t)$ computed by the Gauss-Newton method. The resulting quaternion $\mathbf{r}(t)$ is obtained as,

$$ \mathbf{r}(t) = \alpha\mathbf{g}(t) + (1-\alpha)\mathbf{q}(t) $$

where $0 < \alpha < 1, \alpha \in \mathbb{R}$ is the gain of the complementary filter. The gyroscope orientation quaternion $\mathbf{g}(t)$, is obtained by the following numerical integration

$$ \mathbf{g}(t) = \mathbf{r}(t-\delta t) + \dot{\mathbf{g}}(t)\ \delta t, $$

where $\dot{\mathbf{g}}(t)$ is in accordance to Eq. (7). It is worth noting that $\mathbf{g}(t)$ is initialized as $\mathbf{g}(0) = [1\ 0\ 0\ 0]^T$. To have a better estimation, the gyroscope integration relies on the last quaternion computed by the whole algorithm. Further details and information are reported in [38].

Regarding the calibration procedure we use three different methodologies to calibrate each sensor. For the accelerometer we exploit the assumption of having the sum of the outputs equal to the gravity magnitude when the sensor is stable. As a consequence of this, we adjust the bias and scale for each axis. For the gyroscope calibration, we estimate the bias by placing the sensor fixed on a surface; if the sensor is not moving the angular rate has to be zero. Finally, we perform the magnetometer calibration using the algorithm proposed by Merayo *et al.* in [48].

REFERENCES

[1] H. Zhou and H. Hu, "Human motion tracking for rehabilitationa survey," *Biomedical Signal Processing and Control*, vol. 3, no. 1, pp. 1–18, 2008.

[2] M. A. Goodrich and A. C. Schultz, "Human-robot interaction: a survey," *Foundations and trends in human-computer interaction*, vol. 1, no. 3, pp. 203–275, 2007.

[3] A. Bleiweiss, D. Eshar, G. Kutliroff, A. Lerner, Y. Oshrat, and Y. Yanai, "Enhanced interactive gaming by blending full-body tracking and gesture animation," in *ACM Special Interest Group on Computer Graphics and Interactive Techniques Conference (SIGGRAPH ASIA)*, 2010, p. 34.

[4] C. Pacchierotti, D. Prattichizzo, and K. Kuchenbecker, "Cutaneous feedback of fingertip deformation and vibration for palpation in robotic surgery," *IEEE Transactions on Biomedical Engineering*, vol. 63, no. 2, pp. 278–287, 2015.

[5] S. Rao, N. Llombart, E. Moradi, K. Koski, T. Bjorninen, L. Sydanheimo, J. M. Rabaey, J. M. Carmena, Y. Rahmat-Samii, and L. Ukkonen, "Miniature implantable and wearable on-body antennas: towards the new era of wireless body-centric systems," *IEEE Antennas and Propagation Magazine*, vol. 56, no. 1, pp. 271–291, 2014.

[6] H. Fang, Z. Xie, and H. Liu, "An exoskeleton master hand for controlling DLR/HIT hand," in *Proc. IEEE/RSJ International Conference on Intelligent Robots and Systems (IROS)*, 2009, pp. 3703–3708.

[7] M. Zhou and P. Ben-Tzvi, "Rml glovean exoskeleton glove mechanism with haptics feedback," *IEEE/ASME Transactions on Mechatronics*, vol. 20, no. 2, pp. 641–652, 2015.

[8] I. Oikonomidis, N. Kyriazis, and A. Argyros, "Efficient model-based 3d tracking of hand articulations using kinect," in *Proc. British Machine Vision Cconference (BMVC)*, 2011, pp. 101.1–101.11.

[9] C. Qian, X. Sun, Y. Wei, X. Tang, and J. Sun, "Realtime and robust hand tracking from depth," in *Proc. IEEE Conference on Computer Vision and Pattern Recognition*, 2014, pp. 1106–1113.

[10] L. Dipietro, A. M. Sabatini, and P. Dario, "A survey of glove-based systems and their applications," *IEEE Transaction on Systems, Man, and Cybernetics, Part C*, vol. 38, no. 4, pp. 461–482, 2008.

[11] L. K. Simone, N. Sundarrajan, X. Luo, Y. Jia, and D. G. Kamper, "A low cost instrumented glove for extended monitoring and functional hand assessment," *Journal of neuroscience methods*, vol. 160, no. 2, pp. 335–348, 2007.

[12] R. Gentner and J. Classen, "Development and evaluation of a low-cost sensor glove for assessment of human finger movements in neurophysiological settings," *Journal of neuroscience methods*, vol. 178, no. 1, pp. 138–147, 2009.

[13] M. Borghetti, E. Sardini, and M. Serpelloni, "Sensorized glove for measuring hand finger flexion for rehabilitation purposes," *IEEE Transactions on Instrumentation and Measurement*, vol. 62, no. 12, pp. 3308–3314, 2013.

[14] M. Bianchi, N. Carbonaro, E. Battaglia, F. Lorussi, A. Bicchi, D. D. Rossi, and A. Tognetti, "Exploiting hand kinematic synergies and wearable under-sensing for hand functional grasp recognition," in *Proc. IEEE International Conference on Wireless Mobile Communication and Healthcare*, 2014.

[15] D. Roetenberg, H. Luinge, and P. Slycke, "Xsens mvn: full 6dof human motion tracking using miniature inertial sensors," Xsens Motion Technologies BV, Tech. Rep., 01 2009.

[16] A. Gallagher, Y. Matsuoka, and W.-T. Ang, "An efficient real-time human posture tracking algorithm using low-cost inertial and magnetic sensors," in *Proc. IEEE/RSJ International Conference on Intelligent Robots and Systems (IROS)*, vol. 3, 2004, pp. 2967–2972.

[17] G. Santaera, E. Luberto, A. Serio, M. Gabiccini, and A. Bicchi, "Low-cost, fast and accurate reconstruction of robotic and human postures via imu measurements," in *Robotics and Automation (ICRA), 2015 IEEE International Conference on*. IEEE, 2015, pp. 2728–2735.

[18] A. M. Sabatini, "Estimating three-dimensional orientation of human body parts by inertial/magnetic sensing," *Sensors*, vol. 11, no. 2, pp. 1489–1525, 2011.

[19] J. L. Hernandez-Rebollar, N. Kyriakopoulos, and R. W. Lindeman, "The acceleglove: a whole-hand input device for virtual reality," in *Proc. ACM Special Interest Group on Computer Graphics and Interactive Techniques Conference (SIGGRAPH)*, 2002, p. 259.

[20] Y. S. Kim, B. S. Soh, and S. Lee, "A new wearable input device: Scurry," *IEEE Transaction on Industrial Electronics*, vol. 52, no. 6, pp. 1490–1499, 2005.

[21] H. G. Kortier, V. I. Sluiter, D. Roetenberg, and P. H. Veltink, "Assessment of hand kinematics using inertial and magnetic sensors," *Journal of Neuroengineering and Rehabilitation*, vol. 11, no. 1, p. 70, 2014.

[22] J. Lieberman and C. Breazeal, "Tikl: Development of a wearable vibrotactile feedback suit for improved human motor learning," *IEEE Transaction on Robotics*, vol. 23, no. 5, pp. 919–926, 2007.

[23] S. Scheggi, A. Talarico, and D. Prattichizzo, "A remote guidance system for blind and visually impaired people via vibrotactile haptic feedback," in *Proc. IEEE Control and Automation (MED), 22nd Mediterranean Conference of*, 2014, pp. 20–23.

[24] R. E. Schoonmaker and G. L. C. Cao, "Vibrotactile force feedback system for minimally invasive surgical procedures," in *Proc. IEEE International Conference on Systems, Man and Cybernetics*, vol. 3, 2006, pp. 2464–2469.

[25] S. Scheggi, F. Morbidi, and D. Prattichizzo, "Human-robot formation control via visual and vibrotactile haptic feedback," *IEEE Transactions on Haptics*, vol. 7, no. 4, pp. 499–511, 2014.

[26] S. Scheggi, M. Aggravi, F. Morbidi, and D. Prattichizzo, "Cooperative human-robot haptic navigation," in *Proc. IEEE Internetional Conference on Robotics and Automation*, 2014, pp. 2693–2698.

[27] M. Aggravi, S. Scheggi, and D. Prattichizzo, "Evaluation of a predictive approach in steering the human locomotion via haptic feedback," in *Proc. IEEE/RSJ International Conference on Intelligent Robots and Systems (IROS)*, 2015.

[28] D. Prattichizzo, F. Chinello, C. Pacchierotti, and M. Malvezzi, "Towards wearability in fingertip haptics: a 3-dof wearable device for cutaneous force feedback," *IEEE Transactions on Haptics*, vol. 6, no. 4, pp. 506–516, 2013.

[29] A. G. Perez, D. Lobo, F. Chinello, G. Cirio, M. Malvezzi, J. San Martin, D. Prattichizzo, and M. A. Otaduy, "Soft finger tactile rendering for wearable haptics," in *Proc. IEEE World Haptics Conference (WHC)*, 2015, pp. 327–332.

[30] L. Meli, S. Scheggi, C. Pacchierotti, and D. Prattichizzo, "Wearable haptics and hand tracking via an rgb-d camera for immersive tactile experiences," in *Proc. ACM Special Interest Group on Computer Graphics and Interactive Techniques Conference (SIGGRAPH)*, 2014, p. 56.

[31] S. Scheggi, L. Meli, C. Pacchierotti, and D. Prattichizzo, "Touch the virtual reality: using the leap motion controller for hand tracking and wearable tactile devices for immersive haptic rendering," in *ACM Special Interest Group on Computer Graphics and Interactive Techniques Conference (SIGGRAPH)*, 2015, p. 31.

[32] S. Cobos, M. Ferre, M. A. Sánchez-Urán, and J. Ortego, "Constraints for realistic hand manipulation," *Proc. Presence*, pp. 369–370, 2007.

[33] C. Hrabia, K. Wolf, and M. Wilhelm, "Whole hand modeling using 8 wearable sensors: biomechanics for hand pose prediction," in *Proc. ACM International Conference on Augmented Human*, 2013, pp. 21–28.

[34] T. Lisini Baldi, M. Mohammadi, S. Scheggi, and D. Prattichizzo, "Using inertial and magnetic sensors for hand tracking and rendering in wearable haptics," in *Proc. IEEE World Haptics Conference (WHC)*, 2015, pp. 381–387.

[35] J. Lee and T. L. Kunii, "Model-based analysis of hand posture," *IEE Computer Graphics and Applications*, vol. 15, no. 5, pp. 77–86, 1995.

[36] S. Mulatto, A. Formaglio, M. Malvezzi, and D. Prattichizzo, "Using postural synergies to animate a low-dimensional hand avatar in haptic simulation," *IEEE Transaction on Haptics*, vol. 6, no. 1, pp. 106–116, 2013.

[37] I. M. Bullock, J. Borràs, and A. M. Dollar, "Assessing assumptions in kinematic hand models: a review," in *Proc. IEEE Conference on Biomedical Robotics and Biomechatronics*, 2012, pp. 139–146.

[38] D. Comotti, "Orientation estimation based on gauss-newton method and implementation of a quaternion complementary filter," University of Bergamo, Tech. Rep., 01 2011.

[39] K. Minamizawa, H. Kajimoto, N. Kawakami, and S. Tachi, "A wearable haptic display to present the gravity sensation-preliminary observations and device design," in *Proc. IEEE World Haptics Conference (WHC)*, 2007, pp. 133–138.

[40] E. R. Serina, E. Mockensturm, C. Mote, and D. Rempel, "A structural model of the forced compression of the fingertip pulp," *Journal of biomechanics*, vol. 31, no. 7, pp. 639–646, 1998.

[41] M. Srinivasan and K. Dandekar, "An investigation of the mechanics of tactile sense using two-dimensional models of the primate fingertip," *Journal of biomechanical engineering*, vol. 118, no. 1, pp. 48–55, 1996.

[42] J. Z. Wu, R. G. Dong, S. Rakheja, A. Schopper, and W. Smutz, "A structural fingertip model for simulating of the biomechanics of tactile sensation," *Medical engineering & physics*, vol. 26, no. 2, pp. 165–175, 2004.

[43] K.-H. Park, B.-H. Kim, and S. Hirai, "Development of a soft-fingertip and its modeling based on force distribution," in *Robotics and Automation (ICRA), 2003 IEEE International Conference on*, vol. 3. IEEE, 2003, pp. 3169–3174.

[44] R. Mahony, T. Hamel, and J. Pflimlin, "Nonlinear complementary filters on the special orthogonal group," *IEEE Transaction on Automatic Control*, vol. 53, no. 5, pp. 1203–1218, 2008.

[45] S. Madgwick, A. Harrison, and R. Vaidyanathan, "Estimation of imu and marg orientation using a gradient descent algorithm," in *Proc. IEEE International Conference on Rehabilitation Robotics*, 2011, pp. 1–7.

[46] J. L. Marins, X. Yun, E. R. Bachmann, R. McGhee, and M. J. Zyda, "An extended kalman filter for quaternion-based orientation estimation using marg sensors," in *Proc. IEEE/RSJ International Conference on Intelligent Robots and Systems (IROS)*, vol. 4, 2001, pp. 2003–2011.

[47] H. Z. Tan, M. A. Srinivasan, C. M. Reed, and N. I. Durlach, "Discrimination and identification of finger joint-angle position using active motion," *ACM Transactions on Applied Perception (TAP)*, vol. 4, no. 2, p. 10, 2007.

[48] J. Merayo, P. Brauer, F. Primdahl, J. Petersen, and O. Nielsen, "Scalar calibration of vector magnetometers," *Measurement Science and Technology*, vol. 11, no. 2, p. 120, 2000.

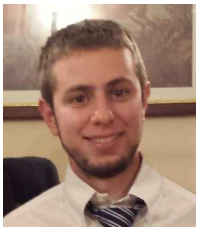

Tommaso Lisini Baldi (S'15) received the B.Sc and M.Sc. degree cum laude in computer and automation engineering in 2011 and 2014 from the University of Siena, Italy. He is currently a Ph.D. student in robotic and automation at the Dept. of Information Engineering and Mathematics of the University of Siena and at the Dept. of Advanced Robotics of the Istituto Italiano di Tecnologia (IIT). His research interests include robotics and haptics focusing on hand tracking, haptics feedback, and motion tracking with inertial sensors. He is a student member of the IEEE.

Stefano Scheggi (S'09 - M'12) received the M.Sc. and Ph.D. degrees in Computer Engineering from the University of Siena, Italy, in 2007 and 2012, respectively. In 2011, he was a Visiting Ph.D. Student at the Department of Computer Science, George Mason University, Fairfax, USA, under the supervision of Prof. Jana Košecká. Since 2012, he held a postdoctoral position at the University of Siena, Italy. Since 2015, he holds a postdoctoral position at the University of Twente, The Netherlands. His research interests include computer vision, mobile robotics, medical robotics, haptics, and augmented/virtual reality. He is a member of the IEEE.

Leonardo Meli (S'13 - M'17) received the M.S. degree in Computer and Automation Engineering and the Ph.D. degree in Information Engineering from the University of Siena, Siena, Italy, in 2012 and 2016, respectively. He was an exchange student at the Karlstad University, Sweden in 2010. He spent the last 4 months of 2015 visiting the BioInstrumentation Laboratory at the Massachusetts Institute of Technology, Cambridge, Ma, USA. His research interests include robotics and haptics focusing on cutaneous force feedback techniques, teleoperation systems for medical applications, and grasping. He is a member of the IEEE.

Mostafa Mohammadi (S'14) received the BSc. and MSc. degrees in electrical engineering-control in 2008, and 2011 from Iran University of Science and Technology, Tehran, Iran. He is currently working toward his Ph.D. degree in robotics and automation at the Department of Information Engineering and Mathematics, University of Siena, Siena, Italy, an at the Department of Advanced Robotics of the Italian Institute of Technology, Genova, Italy. His research interests include grasping, cooperative manipulation, haptics, and aerial robotics. He is a student member of the IEEE.

Domenico Prattichizzo (S'93 - M'95 - SM'15 - F'16) received the M.S. degree in Electronics Engineering and the Ph.D. degree in Robotics and Automation from the University of Pisa in 1991 and 1995, respectively. He is Professor of Robotics at the University of Siena, and since 2009 Scientific Consultant at Istituto Italiano di Tecnoloogia, Italy. In 1994, Visiting Scientist at the MIT AI Lab. His main research interests are in haptics, grasping, visual servoing, mobile robotics and geometric control. Author of more than 200 papers in those fields. From 2013 Chair of the IEEE RAS Early Career Awards Evaluation Panel. Vice-chair for Special Issues of the IEEE Technical Committee on Haptics (2006-2010). Chair of the Italian Chapter of the IEEE RAS (2006-2010), awarded with the IEEE 2009 Chapter of the Year Award. Leader of a research unit in several EU projects. Coordinator of an EU ECHORD-EXPERIMENT, and of an EU IP collaborative project. He is a fellow of the IEEE.